

**ELECTROMAGNETOHYDRODYNAMIC MICROPOLAR-
CASSON FLUID BOUNDARY LAYER FLOW AND HEAT
TRANSFER OVER A STRETCHING MATERIAL
FEATURING TEMPERATURE-BASED THERMOPHYSICAL
PROPERTIES IN A POROUS MEDIUM**

E. O. FATUNMBI¹ AND S. S. OKOYA

ABSTRACT. This study investigates the boundary layer flow and heat transfer analysis in an electromagnetohydrodynamic dissipative micropolar-Casson fluid over a two-dimensional stretching sheet in porous medium. The physical model comprises the impact of thermal radiation, suction/injection, temperature-dependent thermophysical properties (viscosity and thermal conductivity) associated with prescribed surface temperature condition. Appropriate similarity transformation variables are employed to redefine the governing equations from partial into ordinary differential equations while the resultant equations are solved by shooting technique cum Runge-Kutta Fehlberg integration algorithm. The reactions of the physical parameters on the dimensionless quantities are presented through various graphs and tables. From the investigation, it is found out that the skin friction coefficient reduces with growth in the micropolar material and in the presence of electric field terms whereas an opposite trend occurs with a rise in the Casson fluid material and magnetic field terms. More so, there is an increase in the thermal and hydrodynamic boundary layer due to a rise in the electric field and micropolar fluid material parameter. The obtained data in the current study also agree well with existing studies in literature under some limiting conditions.

Keywords and phrases: Micropolar-Casson fluid; Electromagnetohydrodynamic; Temperature-dependent properties; Boundary layer flow; Suction/injection

2010 Mathematical Subject Classification: A80

1. INTRODUCTION

The popularity of the non-Newtonian fluids has continued to abound in the recent times due to their widespread applications in various

Received by the editors September 11, 2021; Revised: November 19, 2021; Accepted: December 03, 2021

www.nigerianmathematicalsociety.org; Journal available online at <https://ojs.ictp.it/jnms/>

¹Corresponding author

fields of human endeavour ranging from sciences, engineering to technology. Such applications are commonly found in polymer engineering, crude oil extrusion, drug manufacturing, food processing, paint rheology, etc. The non-Newtonian fluids are fluids which differ in properties from those of Newtonian (classical) fluids, and thus fall outside the domain of the classical field theories. Unlike the Newtonian fluids which are characterized by linear relationship between the shear stress and shear strain, the viscosity of non-Newtonian fluids is dependent on shear rate or shear rate history and hence, they do not conform to the Newtons law of viscosity. Such fluids include ketchup, butter, cosmetics, polymer solutions, blood, colloids, mud flows and gels. The constitutive models for the non-Newtonian fluids vary due to differences in the fluid characteristics in nature, as such, no single constitutive model can effectively capture the non-Newtonian fluids properties. In the light of this, various models have been formulated to describe the non-Newtonian fluids physical attributes. Some of these models include: Casson fluid, Maxwell fluid, tangent hyperbolic fluid, Johnson-Segalman fluid, Jeffery fluid, micropolar fluid, etc. [1-3].

Prominent among the non-Newtonian fluids is the micropolar fluid formulated by Eringen [4-5]. The concept of micropolar fluid comprises of fluids with rigid, spherical (randomly oriented) particles suspended in a viscous where particles deformation is ignored [6]. The rigid particles contained in a small volume can rotate about the centroid of the volume element. This concept generalizes the Navier-Stokes model and paves way for crucial applications in areas such as slurry technologies, bio mechanics engineering (e.g. cervical flows, blood flow in brain, synovial lubrication, arterial blood flows, etc.), pharmacodynamics (e.g. drug delivery), sediment transport in rivers, etc. [7-8]. Fluids that describes the attribute of micropolar fluids include: colloidal fluids, fluid suspensions, animal blood, liquid crystals, etc. [9-10]. Due to the indispensable applications derivable from the transport of micropolar fluid various researchers have investigated such fluids on different configurations considering different parameters. Mishra et al. [11] numerically studied hydromagnetic reactive micropolar fluid flow along an impermeable stretching sheet. It was reported that the skin friction coefficient falls with a rise in the micropolar material term. Rashad, et al. [12] considered micropolar fluid flow over a continuously moving vertical surface in a thermally and solutal stratified medium using

Keller-box method. The authors found that growth in the micropolar term strengthened the viscous drag and improved the heat transfer. For more studies related to this concept (see Mahmoud [13]; Salawu and Fatunmbi [14]; Keimanesh and Aghanajafi, [15]; Fatunmbi and Adeniyani [16]; Fatunmbi et al. [1]).

Moreover, the simplicity of the Casson fluid model among the other non-Newtonian fluids has drawn the attention of many researchers to study such a fluid on various configurations with diverse assumption. This model captures the flow characteristics of a non-Newtonian fluid and accurately predict the flow of blood in arteries at very low shear rate. Casson fluid characterizes a shear thinning fluid which manifests yield stress attribute. It possesses a property of infinite viscosity at zero rate of shear stress and zero viscosity at infinite rate of shear stress Casson [17]. This model describes the rheological behaviour of various ingredients such as paints, lubricants, jelly, tomato sauce, blood, honey, etc. Ahmad et al. [18] discussed Casson fluid transport past a heated stretching sheet in a porous device with non-uniform viscosity via a finite-difference method. The authors pointed out that the surface temperature increased with a rise in the porosity term. An unsteady flow of a dissipative magneto-Casson nanofluid with convective heat transfer, thermal radiation over a stretching vertical surface plate was scrutinized by Shit and Mandal [19]. The analysis showed that the Casson fluid term caused a resistance to the fluid motion due to a rise in the viscosity. Fatunmbi and Okoya [20] numerically analyzed the impact of quadratic Boussinesq approximation and variable thermal conductivity in a stagnation point flow of Casson fluid. The authors reported that the Casson fluid material term enhanced both the thermal field and the viscous drag. Recently, Omotola and Fatunmbi [21] studied the motion of a radiative Casson fluid over a convectively heated permeable material with Joule heating and slip effects.

The attention of researchers and scientists have been drawn to the consequential engineering and manufacturing applications of magnetohydrodynamic in various fields. This phenomenon is frequently encountered in nuclear reactors, electric power generation devices, MHD generators and accelerators/or MHD thrusters, boundary layer control in aerodynamics, etc. [22]. Magnetohydrodynamic deals with the interaction of electrically conducting fluid (e, g. salt water, liquid metals and plasmas with magnetic field [23-24] while studying the combined effects of electric and magnetic fields on the

flow and heat transfer of nanofluid noticed that the fluid velocity accelerated with high values of electric field while it decelerated with magnetic field parameter. Aliy and Kishan [25] analytically inspected the flow of an electrical magnetohydrodynamic Williamson fluid over a convectively heated sheet with uneven thickness. The process of suction/injection has been found to be dominant in various engineering processes such as the design of radial diffusers, thrust bearing and thermal oil recovery. Fluid flow and heat transfer can be easily altered in the presence of suction/injection. Suction has been found to enhance the skin friction whereas injection acts otherwise. In view of the applications of such a concept, Rohni et al. [26] studied laminar, steady two-dimensional flow and heat transfer of a Newtonian fluid with buoyancy force over a shrinking sheet with suction effect. Fatunmbi et al. [1] evaluated the flow and heat transfer characteristics of micropolar fluid over an inclined nonlinearly stretched sheet with suction/injection processes whereas Ullah et al. [27] investigated an incompressible flow of a tangent hyperbolic fluid featuring wall suction/injection effects.

The mixture of the micropolar and Casson fluid has been found to be useful in bio-engineering activities, food processing, production of pharmaceutical products, paints, synthetic lubricants, biological fluids. Such a blend was investigated by Mehmood et al. [28] over a convectively heated stretching surface featuring internal heat source. Iqbal et al. [29] conducted a research with such a composition featuring an inclined magnetic field and viscous dissipation. Nevertheless, there has not been a study with the mixture of micropolar and Casson fluid encompassing the combined effects of magnetic and electric fields with temperature-dependent viscosity and thermal conductivity over a permeable material surface to the best of the authors knowledge. For accurate prediction of flow and heat transfer characteristics in the flow region and coupled with the consequential applications, it is necessary to investigate such a phenomenon.

Therefore, the focus of the present study is to investigate the combined effects of magnetic and electric fields in the boundary layer flow and heat transfer of micropolar-Casson fluid over a two-dimensional stretching sheet with temperature-based viscosity, thermal conductivity, suction/injection processes, viscous dissipation and internal heat generation. The boundary layer equations of the fluid flow consist of the continuity equation, the momentum

equation, and energy equation derived in view of Maxwell equation and Ohms law in the presence of electrical magnetohydrodynamic (EMHD). A prescribed surface temperature (PST) heating condition is applied in the heat equation in the presence of weak concentration of micropolar rigid particles. A numerical method via shooting technique alongside Runge-Kutta Fehlberg scheme is employed to solve the outlining equations while the results are presented in tables and graphs with appropriate discussion

2. PROBLEM DEVELOPMENT

The development of the partial differential equations for the electromagnetohydrodynamic flow and heat transfer in a micropolar-Casson fluid is carried out with the assumptions that: the flow is steady, incompressible in a two-dimensional linearly stretching sheet in a saturated porous medium. The axes of the sheet are taken to be $(x, y, 0)$ with the flow being measured in x direction along the stretching surface while y axis is normal to it. The respective velocity components are u and v as illustrated in Figure. 1. External magnetic and electric fields of uniform strength are applied normal to the flow direction without accounting for the impact of the induced magnetic field and Hall current due to significantly low Reynolds number. The fluid thermophysical properties such as the viscosity and thermal conductivity are assumed to be linearly dependent on temperature while the other fluid properties are assumed to be constant. The velocity of the linearly stretching sheet is taken as $u = u_w = bx$ where b is the stretching rate greater than zero, the wall suction/injection is considered to be $v = v_w$. A prescribed surface temperature (PST) is assumed for the energy equation with the surface temperature $T_w > T_\infty$. The impact of thermal radiation, viscous dissipation and internal heat source are modelled into the heat equation while the microrotation field is assumed to have weak concentration throughout this study. The stress tensor and couple stress tensor relations for isotropic micropolar fluid are expressed as [3, 4, 6].

$$\tau_{ij} = (-P + \lambda_r v_{k,k}) \delta_{ij} + \mu (v_{i,j} + v_{j,i}) + \beta (v_{j,i} - v_{i,j}) - \beta \epsilon_{kij} \omega_k, \quad (1)$$

$$C_{ij} = c_o \omega_{k,k} \delta_{ij} + c_d (\omega_{i,j} + \omega_{j,i}) + c_a (\omega_{i,j} - \omega_{j,i}), \quad (2)$$

where τ_{ij} is the Cauchy stress tensor, P is the pressure, λ_r and μ are second viscosity coefficient and dynamic viscosity respectively. also, β is the dynamic microrotation/vortex viscosity, c_o , c_a and c_d are the coefficients of angular viscosity, v_i , ω_k and ϵ_{ijk} are the

velocity component, angular velocity component and the alternating/permutation stress tensor, C_{ij} is the couple stress tensor, δ_{ij} is the usual Kronecker delta. In a similar manner, the rheological equation of an isotropic, incompressible flow of Casson fluid is specified as [30-32].

$$G_{ij} = \left(\mu_b + \frac{P_y}{\sqrt{2\pi}} \right) 2e_{ij}; \pi > \pi_c, \quad G_{ij} = \left(\mu_b + \frac{P_y}{\sqrt{2\pi_c}} \right) 2e_{ij}; \pi < \pi_c, \quad (3)$$

where G_{ij} denotes the Cauchy stress tensor, P_y stands for the yield stress of the fluid described as $P_y = \frac{\mu_B \sqrt{2\pi}}{\gamma}$. The plastic dynamic viscosity of the non-Newtonian fluid is described as μ_b while π depicts the product of deformation rate with itself ($\pi = e_{ij}e_{ij}$), π_c indicates the critical value of the product of the component of the deformation rate with itself which is based on the non-Newtonian model. The fluid viscosity can also be expressed as $\mu = \mu_b + \frac{P_y}{\sqrt{2\pi}}$. Thus, in view of P_y , the fluid viscosity becomes $\mu = \mu_b \left(1 + \frac{1}{\gamma} \right)$ where $\gamma = \mu_b \frac{\sqrt{2\pi}}{P_y}$ describes the Casson fluid parameter.

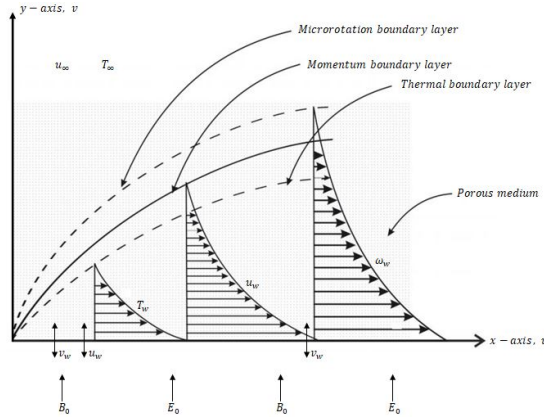


Fig. 1 Flow Geometry

Taking cognizance of the aforementioned assumptions coupled with boundary layer approximation with the condition of temperature-based viscosity, and variable thermal conductivity, wall suction/injection, viscous dissipation and porosity of the medium, the governing equations of the mass conservation, momentum and energy equations are specified as follows [28, 32].

$$\frac{\partial u}{\partial x} + \frac{\partial v}{\partial y} = 0, \quad (4)$$

$$u \frac{\partial u}{\partial x} + v \frac{\partial u}{\partial y} = \frac{1}{\rho_\infty} \left[\left(1 + \frac{1}{\gamma} \right) \frac{\partial}{\partial y} \left(\mu_b \frac{\partial u}{\partial y} \right) \right] + \frac{\beta}{\rho_\infty} \frac{\partial^2 u}{\partial y^2}$$

$$+\frac{\beta}{\rho_{\infty}}\frac{\partial\omega}{\partial y}+f_b, \quad (5)$$

$$u\frac{\partial\omega}{\partial x}+v\frac{\partial\omega}{\partial y}=\frac{H}{\rho j}\frac{\partial^2\omega}{\partial y^2}-\frac{\beta}{\rho_{\infty}j}\left(2\omega+\frac{\partial u}{\partial y}\right), \quad (6)$$

$$u\frac{\partial T}{\partial x}+v\frac{\partial T}{\partial y}=\frac{1}{\rho_{\infty}c_p}\frac{\partial}{\partial y}\left[\left(k(T)+\frac{16T_{\infty}^3\sigma^*}{3k^*}\right)\frac{\partial T}{\partial y}\right]+\frac{B^*}{\rho_{\infty}c_p}(T-T_{\infty})$$

$$+\frac{1}{\rho_{\infty}c_p}\left[\mu(T)\left(1+\frac{1}{\gamma}\right)+\beta\right]\left(\frac{\partial u}{\partial y}\right)^2. \quad (7)$$

Eqs. (4-6) are subject to boundary conditions specified as:

$$y=0: u=u_w=bx, v=v_w, \omega=-s\frac{\partial u}{\partial y}, T=T_w=(T_{\infty}+Ax^{\kappa})$$

$$y\rightarrow\infty: u\rightarrow 0, \omega\rightarrow 0, T\rightarrow T_{\infty}, \quad (8)$$

where f_b , the last term in Eq. (5) denotes some body forces. Also, u and v are component of velocities in x and y directions respectively, b is the stretching rate, ρ defines the fluid density, β represents vortex viscosity, T is the fluid temperature, ω is the component of microrotation, j is the microinertia density, c_p is the specific heat at constant pressure, H describes the spin gradient viscosity, B^* is the coefficient of heat generation/absorption and k_p is the permeability of the porous medium. More so, subscript w/∞ signifies wall/infinity condition, s is a surface boundary parameter with the interval $0 \leq s \leq 1$. The case when $s = 0$ corresponds to $\omega = 0$, this represents no-spin condition i.e. strong concentration such that the micro-particles close to the wall are unable to rotate. The case $n = \frac{1}{2}$, indicates weak concentration of micro-particles and the vanishing of anti-symmetric part of the stress tensor and the case $s = 1$ represents turbulent boundary layer flows [33-34].

Analysis is carried out for the various body force to which the micropolar-Casson fluid is subjected as (i) Electromagnetohydrodynamic force (EMHDF) (ii) Darcy force (DF). The Lorentz force per unit mass is stated as

$$\frac{1}{\rho_{\infty}}(\mathbf{J} \times \mathbf{B}), \quad (9)$$

where

$$\mathbf{J} = \sigma(\mathbf{E} + \mathbf{V} \times \mathbf{B}). \quad (10)$$

In the preceding equation, $\mathbf{E} = (0, 0, -E_0)$ denotes the transverse electric field, $\mathbf{B} = (0, B_0, 0)$ represents magnetic field vector, $\mathbf{V} = (u, v, 0)$ connotes velocity field while \mathbf{J} is the current density. In

view of Eqs. (10), the applied electric and magnetic fields Eq. (9) reduces to

$$\frac{\sigma}{\rho_\infty} (B_0 E_0 - B_0^2 u). \quad (11)$$

Likewise, the Darcy force per unit mass is expressed as

$$-\frac{\mu_b}{\rho_\infty k_p} \mathbf{V} = -\frac{\mu_b}{\rho_\infty k_p} (u, v, 0) = \left(-\frac{\mu_b}{\rho_\infty k_p} u, -\frac{\mu_b}{\rho_\infty k_p} v, 0 \right). \quad (12)$$

Where the minus sign connotes the draglike opposing force. In view of boundary layer assumption, the Darcy force Eq. (12) can be expressed as

$$-\frac{\mu_b}{\rho_\infty k_p} \mathbf{V} = -\frac{\mu_b}{\rho_\infty k_p} (u, v, 0) = \left(-\frac{\mu_b}{\rho_\infty k_p} u, 0, 0 \right). \quad (13)$$

Now combining Eqs. (11) and (13), the body force f_b can now be expressed as

$$f_b = \frac{\sigma}{\rho_\infty} (B_0 E_0 - B_0^2 u) - \frac{\mu_b}{\rho_\infty k_p} u. \quad (14)$$

The viscosity μ_b and the thermal conductivity k vary linearly with temperature as considered by Layek et al. [35]; Akinbobola and Okoya [36]; Opadiran and Okoya [37]. The respective variation of the viscosity μ_b and the thermal conductivity k are expressed in Eq. (15) as

$$\mu_b(T) = \mu_{b_\infty} [1 + a(T_w - T)], \quad k(T) = k_\infty [1 + c(T - T_\infty)]. \quad (15)$$

3. THE TRANSFORMED EQUATIONS

Introducing similarity transformations variables and dimensionless quantities (16) into the governing equations (4-7) leads to the automatic satisfaction of the continuity equation (4).

$$\begin{aligned} \eta = y \left(\frac{b}{\nu} \right)^{1/2}, \quad \psi = f(\eta) x (b\nu)^{1/2}, \quad \omega = bxg(\eta) \left(\frac{b}{\nu} \right)^{1/2}, \quad u = \frac{\partial\psi}{\partial y}, \\ v = -\frac{\partial\psi}{\partial x}, \quad \theta = \frac{T - T_\infty}{T_w - T_\infty}, \quad Ec = \frac{u_w^2}{c_p(T_w - T_\infty)}, \quad Q = \frac{B^*}{b\rho c_p}, \quad M = \frac{\sigma B_0^2}{b\rho_\infty}, \\ \varepsilon = c(T_w - T_\infty), \quad R = \frac{\beta}{\mu_b}, \quad Da = \frac{\nu}{bk_p}, \quad Pr = \frac{\mu_\infty c_p}{k_\infty}, \quad \delta = a(T_w - T_\infty), \\ E_1 = \frac{E_0}{B_0 u_w}, \quad Nr = \frac{16\sigma^* T_\infty^3}{3k^* k}, \quad fw = -\frac{v_w}{\sqrt{b\nu}}. \end{aligned} \quad (16)$$

In view of Eq. (16), the momentum, microrotation and energy Eqs. (5-7) transform to the underlisted ordinary differential equations:

$$\left[\left(1 + \frac{1}{\gamma} \right) (1 + \delta - \delta\theta) + R \right] f''' - \left(1 + \frac{1}{\gamma} \right) \delta\theta' f'' + Rg' - f'^2 - (Mf' - E_1) + ff' - \left[Da \left(1 + \frac{1}{\gamma} \right) (1 + \delta - \delta\theta) + R \right] f' = 0, \quad (17)$$

$$(1 + R/2) g'' + fg' - f'g - R(2g + f'') = 0, \quad (18)$$

$$(1 + \varepsilon\theta + Nr) \theta'' + \varepsilon\theta'^2 + Pr(f\theta' - \kappa f'\theta) + PrQ\theta + PrEc \left[\left(1 + \frac{1}{\gamma} \right) (1 + \delta - \delta\theta) + R \right] f''^2. \quad (19)$$

Likewise, the boundary conditions (8) transform to:

$$\begin{aligned} f'(0) = 1, \quad f(0) = fw, \quad g = sf''(0), \quad \theta(0) = 1 \\ f'(\infty) = 0, \quad \theta(\infty) = 0, \quad g(\infty) \rightarrow 0. \end{aligned} \quad (20)$$

4. THE QUANTITIES OF ENGINEERING INTEREST

The quantities useful for the engineering community in this study are the skin friction coefficient and the local Nusselt number (which correspond to heat transfer at the surface of the sheet). These quantities are sequentially stated in Eq. (21) as:

$$C_{fx} = \frac{H_w}{\rho_\infty u_w^2}, \quad Nu_x = \frac{xq_w}{k(T_w - T_\infty)}, \quad (21)$$

where H_w indicates the shear stress while q_w defines the heat flux at the surface. Where

$$H_w = \left(\mu + \frac{P_y}{\sqrt{2\pi_c}} + \beta \right) + \beta\omega \Big|_{y=0}, \quad q_w = - \left(k_\infty + \frac{16T_\infty^3 \sigma^*}{3k^*} \right) \frac{\partial T}{\partial y} \Big|_{y=0}. \quad (22)$$

The non-dimensional forms of Eq. (21) in view of Eq. (16) are respectively expressed in (23-24) as:

$$C_{fx} = \left[\left(1 + \delta - \delta\theta + \frac{1}{\gamma} \right) + R(1 - s) \right] Re_x^{-1/2} f''(0), \quad (23)$$

$$Nu_x = - [1 + Nr(1 + \theta(0))] Re_x^{1/2} \theta'(0). \quad (24)$$

5. NUMERICAL METHOD WITH VALIDATION

Owing to the nonlinearity of the governing equations, the analytical solution is not feasible, hence a numerical solution is sought to tackle the set of Eqs. (17-19) subject to the boundary conditions (20). The shooting technique is adopted alongside Runge-Kutta-Fehlberg algorithm. The detail of this method can be found in the studies of Fatunmbi et al. [1]; Mabood and Das [38]; Mahanthesh et al. [39] and Attili [40]. To carry out the parametric computations, the physical parameters have been subjected to the following default values $fw = 0.3, \gamma = 0.1, R = E_1, M = Da = 0.5, Nr = \varepsilon = Q = \delta, 0.2, Ec = 0.1, s = 0.5$ and $Pr = 0.7$ unless otherwise specified in the graphs. The accuracy of the numerical code developed is authenticated by direct comparison of the obtained data with some related published studies under limiting conditions as depicted in Tables 1 and 2.

Table 1. Comparison of the values of Nu_x with existing works for various values of Pr

Pr	Chen [41]	Qasim et al. [42]	Present study
0.72	0.46170	0.46360	0.46368
1.00	0.58010	0.58202	0.58211
3.00	1.16525	1.16525	1.16535
5.00	1.56805	1.56805	1.56816
7.00	1.89540	1.89542	1.89551
10.00	2.30800	2.30800	2.30811
100.00	7.76565	7.75826	7.76576

Table 1 records the comparison of the Nusselt number Nu_x gotten in this study with the works of Chen [41] and Qasim et al. [42] for different values of Prandtl number Pr when $R = Ec = Nr = Da = M = \varepsilon = \delta = Q = 0$ and $\gamma \rightarrow 0$. Likewise, Table 2 reveals the comparison of the skin friction coefficient C_{fx} in the current study with the studies of Kumar [43] and Tripathy et al. [44] under limiting conditions. It is worthy to state that both tables show evidence of good agreement with the published works which confirm the accuracy and validity of the present numerical code.

Table 2. Comparison of the values of C_{fx} with published studies of Kumar [43] and Tripathy et al. [44] for variation in R, M and Da

R	M	Da	Kumar [43]	Tripathy <i>et al.</i> [44]	Present study
0.0	0.0	0.0	1.000000	1.000008	1.0000084
0.5	0.0	0.0	0.880200	0.901878	0.8994515
0.5	1.0	0.0	1.209900	1.250358	1.2496132
0.5	1.0	1.0	-	1.510062	1.5127320
0.0	0.5	0.0	1.189000	1.225590	1.2257448
1.0	0.5	0.0	0.997600	0.995088	0.9919970
1.0	0.5	1.0	-	1.2651260	1.2646592

5. RESULTS AND DISCUSSION

In this section, the reactions of the dimensionless quantities, namely: velocity, temperature, microrotation as well as skin friction coefficient and Nusselt number for variations in the physical parameters are analyzed and discussed.

5.1. Parameters effects on the quantities of engineering interest

Firstly, the impacts of some selected parameters on the skin friction coefficient C_{fx} and on Nusselt number Nu_x (heat transfer) are analyzed in this sub-section. As displayed in Table 3, the impacts of the Casson fluid material parameter γ , micropolar material parameter R , magnetic field term M , electric field parameter E_1 and suction/injection parameters fw are checked on C_{fx} and Nu_x . It is clearly shown in this the table that the parameters γ, M and $fw > 0$ compels a rise in the skin friction coefficient C_{fx} whereas a rise in R, E_1 and $fw < 0$ act in opposite manner. The micropolar fluid as well as injection processes with the imposition of electric field are suitable for the reduction of the skin friction coefficient. Conversely, there is need to reduce the magnitudes of the magnetic field term, Casson fluid material and suction term to achieve the lowering of the skin friction coefficient C_{fx} . The heat transfer (Nu_x) on the other hand improves by the enhancement of R, E_1 and $fw > 0$. Hence, to improve the transfer of heat across the surface of the sheet, the magnitudes of these parameters can be increased to achieve this aim. On the contrary, the magnetic field term as well as injection processes and Casson fluid material term decrease the rate of heat transfer across the surface as noted from Table 3.

Table 3. Computational values of C_{fx} and Nu_x for variations in γ, R, M, E_1 and fw

γ	R	M	E_1	fw	C_{fx}	Nu_x
0.1					0.4117690	0.4641380
0.3	0.2	0.2	0.1	0.1	0.6118637	0.4503395
0.5					0.7280033	0.4304351
	0.5				0.4003802	0.4696632
0.2	1.0				0.3470127	0.4948168
	1.5				0.3241945	0.5049020
		0.1			0.4046095	0.4673025
	0.2	0.3			0.4326948	0.4547534
		0.5			0.4658516	0.4395527
			0.0		0.4157337	0.4606570
		0.2	0.5		0.3960065	0.4773477
			0.8		0.3842833	0.4865931
				0.0	0.4063492	0.4299083
		0.1	0.3		0.4225575	0.5355460
				0.7	0.4439353	0.6887157
				-0.1	0.4009127	0.3967346
				-0.3	0.3790264	0.2757287
				-0.6	0.3735312	0.2486793

5.2. Parameters effects on velocity, temperature & microrotation fields

Here, various graphs are plotted to illustrate the effects of different physical parameters on the dimensional quantities. The impact of electric field parameter E_1 in the presence of the Darcy parameter Da is illustrated in Fig. 2. Increasing the magnitude of E_1 raises the fluid motion as there is an expansion of the hydrodynamic boundary layer structure. As noted in Table 3, the skin friction coefficient reduces as E_1 rises, this trend stirs up an accelerating force which reduces the frictional resistance and thereby leads to a rise in the streamline far from the stretching surface. Such phenomenon improves the accelerating body force to the flow and consequently raises the fluid velocity. However, a rise in the Darcy number creates a resistance to the fluid motion and as such, there is a reduction in the velocity profile as depicted in Fig. 2. Figure 3 displays the effect of the Casson fluid term γ and material micropolar term R on the velocity profile. There is decelerated flow with a rise in γ whereas an increase in the strength of R improves the fluid motion. Basically, a rise in γ enhances the viscosity of the

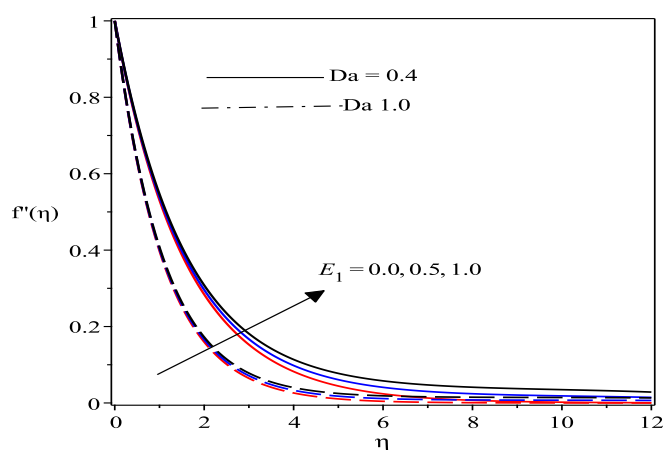


Fig. 2. Effect E_1 and Da on velocity profile

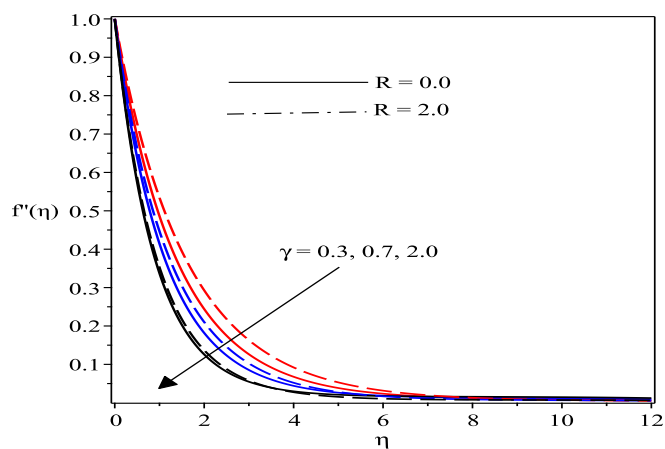


Fig. 3. Impact of γ and R on temperature

fluid and consequently creates resistance to the fluid motion leading to a decelerated flow as seen in this figure. This trend reveals that rising values of γ dictates a fall in the velocity field owing to a decrease in the yield stress as γ rises which in turn decelerates the motion of the fluid. Besides, an enhancement in γ raises the plastic dynamic viscosity over that of the Casson fluid and in such a situation, the fluid motion is reduced. However, the hydrodynamic boundary layer grows with an increase in R . A rise in R implies a reduction in the dynamic viscosity but a rise in the vortex viscosity β and in consequence, the viscous force is reduced such that the fluid motion appreciates. Meanwhile, the influence of γ and R

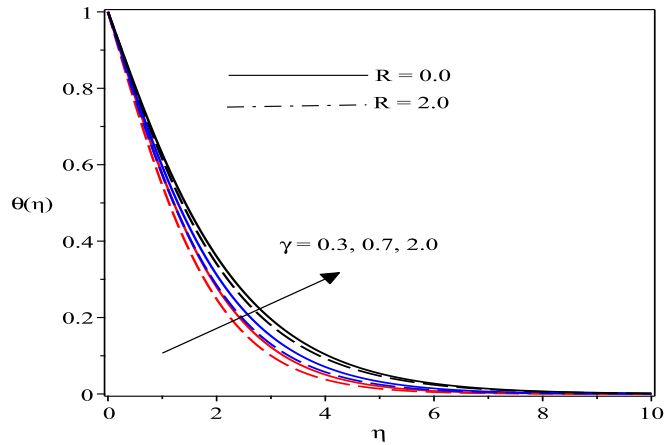


Fig. 4. Effects γ and R on temperature field

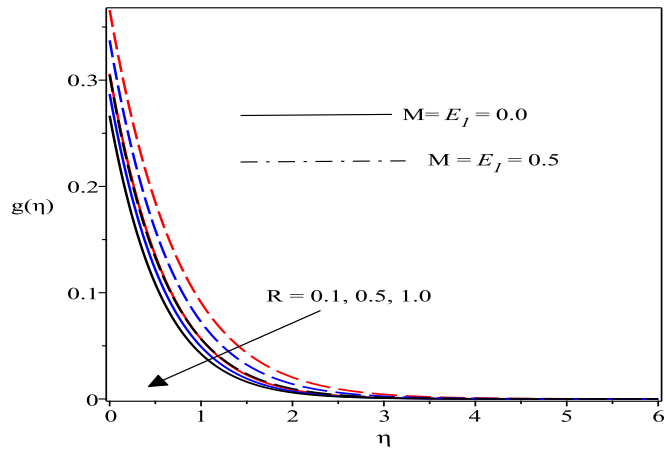


Fig. 5. Impact of R on microrotation profile

on the temperature field however shows a converse trend to that of velocity profile as demonstrated in Fig. 4. The thermal boundary layer rises with an increase in γ and in consequence, the temperature distribution is improved. The resistance to the fluid motion as a result of the fluid viscosity generates a frictional heating in the flow field and thus provides additional heating leading to a rise in temperature. Figure 5 reveals that a rise in material micropolar parameter R reduces the microrotation profile in the presence or otherwise of the magnetic and electric fields but the presence of magnetic and electric fields raises the microrotation boundary layer as observed in this figure. Figure 6 and 7 illustrate the responses

of the velocity and temperature fields for variations in the viscosity parameter δ . Increasing the magnitude of δ enables the fluid to be more viscous and thereby offers a drag in the fluid motion leading a decelerated flow as noticed this figure. Meanwhile, a frictional heating is created due to the drag created in the fluid motion by rising viscosity and consequently the surface temperature is raised as demonstrated in Fig. 7. Hence, a rise in δ makes the thermal boundary layer structure to be enlarged and enhance the temperature as well. Figures 8 and 9 display the effects of injection and

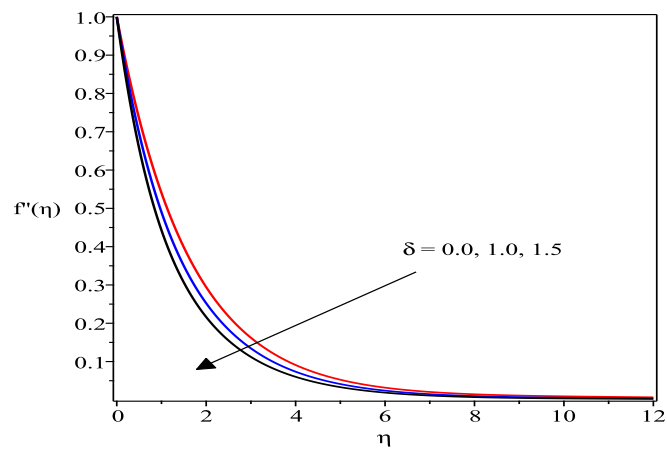


Fig. 6. Effect of δ on velocity profile

suction on the temperature profiles. From Fig. 8, a rise in injection boosts the thermal field and causes the surface temperature to rise. On the other hand, the impact of suction is to lower the temperature distribution as noticed in Fig. 9. The physical reason for this can be attributed to the fact that the Casson-micropolar fluid is brought closer to the surface such that it reduces the thermal boundary layer thickness leading to reduction in the temperature distribution within the boundary layer. Figure 10 describes the variation of temperature profiles with η for different values of Eckert number Ec . The positive Eckert number applies to cooling the sheet which is an indication of heat loss from the stretching sheet to the fluid. It is clear that increasing values of Ec enhances temperature distribution. This response is due the fact that as Ec increases, heat is generated as a result of the drag between the fluid particles. The internal heat generation inside the fluid increases the bulk fluid temperature which is an indication of additional heating in the flow region due to viscous dissipation, thus, this additional heat causes

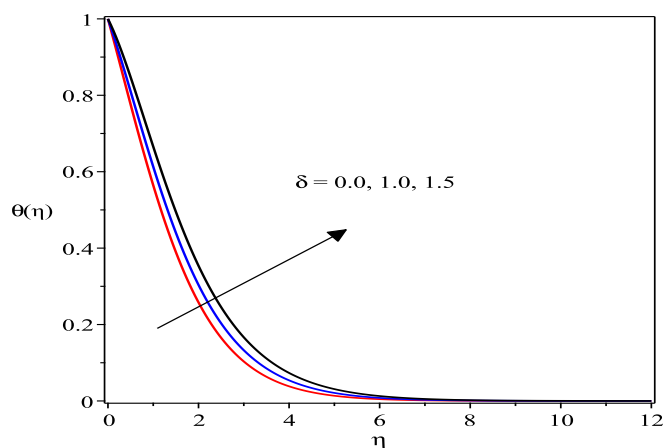


Fig. 7. Graph of δ on temperature

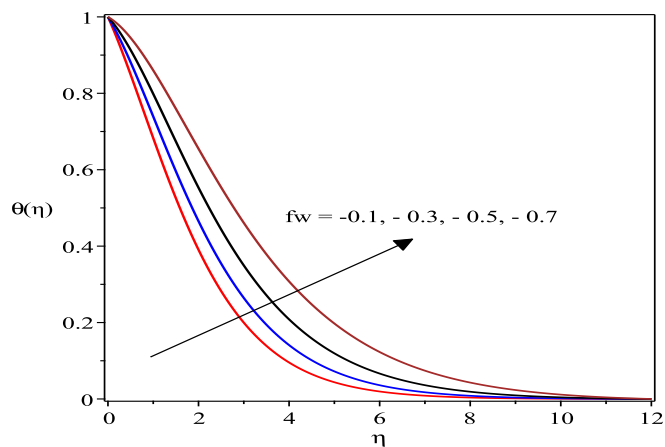


Fig. 8. Impact $fw < 0$ on temperature

an increase in the fluid temperature. On the other hand, the influence of the temperature exponent term κ is to reduce the magnitude of the temperature as clearly demonstrated in Fig. 11. A rise in κ shrinks the thermal boundary layer and consequently reduces the average temperature as noticed in this figure. Figure 12 illustrates the impact of the thermal conductivity parameter ε on the thermal field. A rise in ε raises the surface temperature owing to a boost in the thermal condition. The influence of heat source parameter Q on the temperature profiles is captured in Fig. 13. It is clear from this plot that the thermal boundary layer thickness increases with a rise in the magnitude of Q . This is due to the fact that

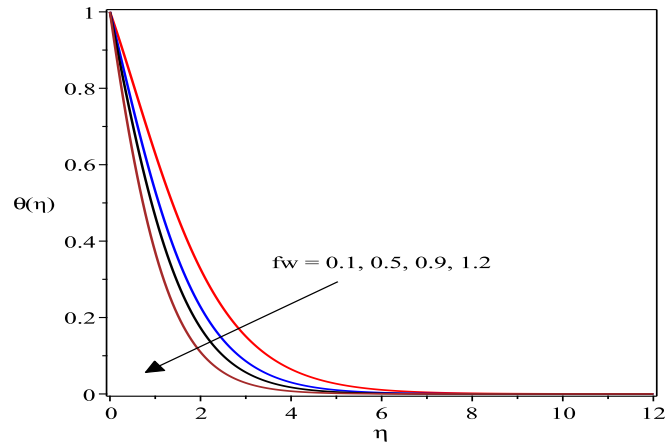


Fig. 9. Plot of $fw > 0$ on temperature

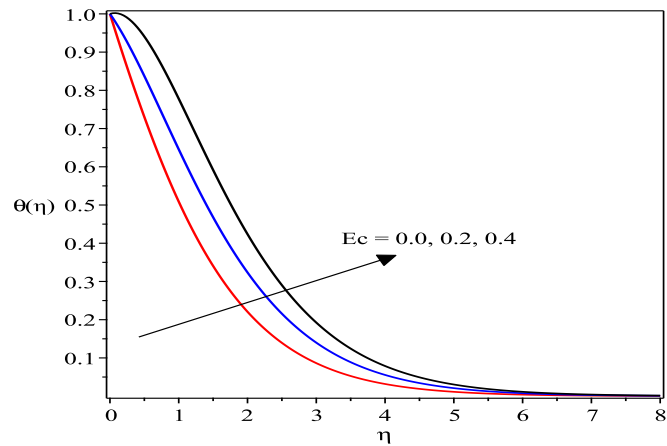


Fig. 10. Effect of Ec on temperature

energy is generated by the imposition of Q leading to a rise in the Casson-micropolar fluid temperature. The dimensionless velocity for different values of the magnetic field M is plotted in Fig. 14. It is noticeable that velocity of the micropolar-Casson fluid reduces with the intensification of the strength of M . The impact of the transverse externally applied magnetic field to an electrically conducting micropolar-Casson fluid generates a retarding force (Lorentz force). This force creates a resistance in the fluid motion. The magnetic field exerts draglike force on the fluid flow and thereby causes the skin friction coefficient within the boundary layer vicinity to rise as discussed in Table 3. However, as M increases, the drag force

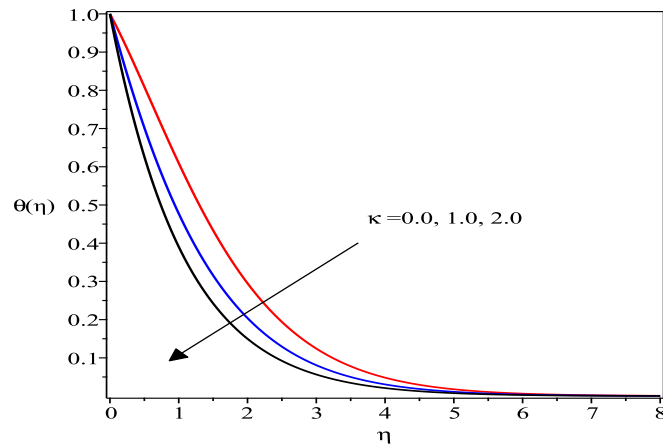


Fig. 11. Response of κ on temperature

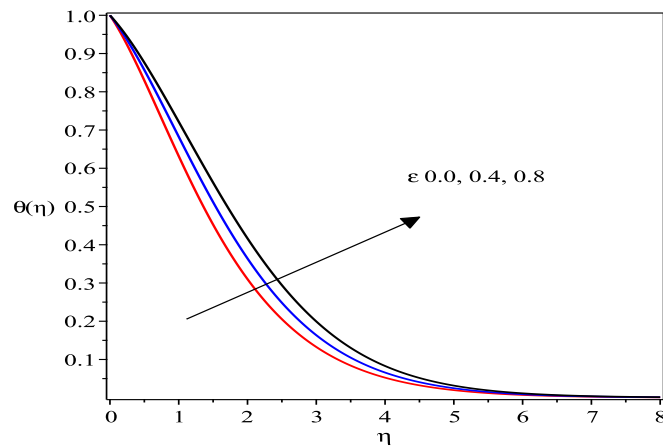


Fig. 12. Influence of ε on temperature

also rises leading to additional heating in the vicinity of the boundary layer. In view of this, there is a rise in the temperature of the micropolar-Casson fluid as demonstrated in Fig. 15.

6. CONCLUDING REMARKS

A mathematical model has been developed to investigate the boundary layer flow and heat transfer phenomenon in electromagnetic hydrodynamic micropolar-Casson fluid over a two-dimensional stretching material in a porous medium. The flow equations features the impacts of variable viscosity and thermal conductivity, suction/injection, viscous dissipation, heat source/sink with prescribed

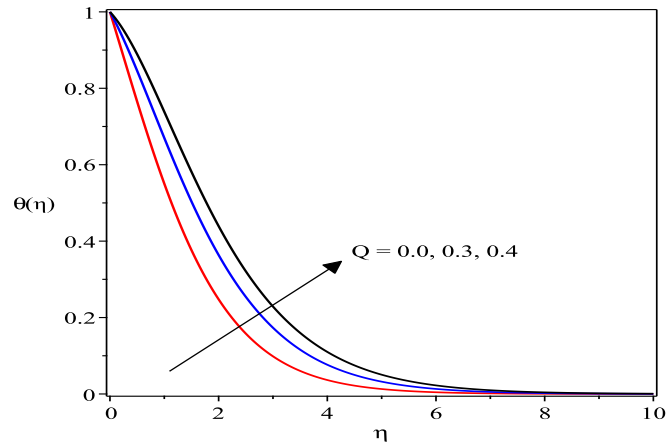


Fig. 13. Impact of Q on temperature

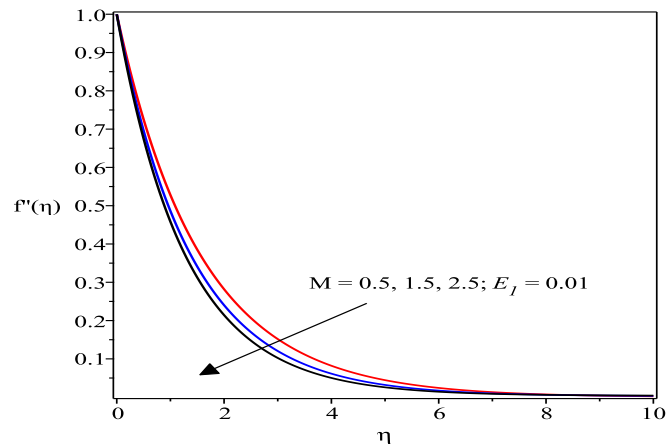


Fig. 14. Effect of M on velocity field

surface temperature heating condition. The main equations are translated from partial to ordinary differential equations using relevant similarity transformation variables and afterward solved via shooting technique alongside Runge-Kutta Fehlberg integration scheme. The data obtained from the analysis are validated with existing relevant studies in literature and found to be in good agreement. Various graphs and tables have been sketched to illustrate the effects of the various physical parameters on the dimensionless quantities. Summarily, it is deduced from this study that:

- The electric field boosts the hydrodynamic boundary layer and enhances the fluid motion whereas the magnetic field,

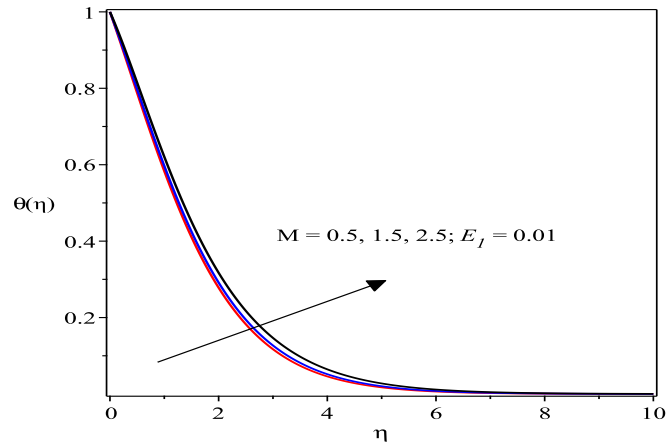


Fig. 15. Impact of M on temperature profile

Casson fluid material and Darcy parameters causes a decline in the motion of the fluid.

- The skin friction coefficient can be drastically reduced by applying micropolar fluid in the presence of electric field and injection processes whereas the Casson fluid material term, magnetic field term and suction processes strengthen the skin friction coefficient.
- Heat transfer improves in the presence of the Casson fluid, micropolar material term, electric field and suction while such a trend is reversed with the imposition of the magnetic field and suction terms.
- There is an enlargement in the thermal boundary layer structure as well as surface temperature with growth in the magnitude of thermal conductivity term, Eckert number, magnetic field term as well heat source in the presence of these parameters.

ACKNOWLEDGEMENTS

The authors would like to thank the anonymous referees whose comments improved the original version of this manuscript.

Table 4. NOMENCLATURE

Symbols	description
u, v	Velocity in x, y direction
T	Temperature
ν	kinematic viscosity
B_0	magnetic field intensity
ρ	fluid density
s	surface boundary parameter
β	vortex viscosity
k^*	mean absorption coefficient
T_w	wall temperature
Nr	thermal radiation parameter
σ	electrical conductivity
T_∞	upstream temperature
c_p	heat capacity of the fluid
j	micro inertial density
k	thermal conductivity
H	spin gradient viscosity
x, y	cartesian coordinates
B^*	heat generation coefficient
σ^*	Stefan-Boltzmann constant
ε	thermal conductivity parameter
v_w	wall suction/injection
Da	Darcy number
b	stretching constant
δ	viscosity parameter
R	material parameter
Ec	Eckert number
Pr	Prandtl number
E_0	electric field intensity
E_1	electric field parameter
Q	heat source/sink parameter
M	magnetic field parameter
a, c	constants

REFERENCES

- [1] E. O. Fatunmbi, S. S. Okoya and O. D. Makinde, *Convective heat transfer analysis of hydromagnetic micropolar fluid flow past an inclined nonlinear stretching sheet with variable thermophysical properties*, Diffusion Foundation, **26**, 63-77, 2020.
- [2] S. O. Salawu and H. A. Ogunseye, *Entropy generation of a radiative hydromagnetic Powell-Eyring chemical reaction nanofluid with variable conductivity and electric field loading*, Results in Engineering, **5**, 100072, 2020.
- [3] J. Chen, C. Liang and J. D. Lee, *Theory and simulation of micropolar fluid dynamics*. J. Nanoengineering and Nanosystems, **224**, 31-39, 2011.
- [4] A. C. Eringen (1966), *Theory of micropolar fluids*, J. Math. Anal. Appl., **16**, 1-18, 1966.
- [5] A. C. Eringen (1972). *Theory of thermo-microfluids*, Journal of Mathematical Analysis and Applications, **38**, 480-496, 1972.
- [6] G. Lukaszewicz, *Micropolar fluids: Theory and Applications* (1st Ed.). Birkhauser, Boston, 1999.
- [7] M. M. Rahman, M. J. Uddin and A. Aziz, *Effects of variable electric conductivity and non-uniform heat source (or sink) on convective micropolar fluid flow along an inclined flat plate with surface heat flux*, International Journal of Thermal Science **48**, 2331-2340, 2009.
- [8] U. S. Reena and Rana E. Effect of Dust Particles on rotating micropolar fluid heated from below saturating a porous medium, Applications and Applied Mathematics: An International Journal, **4**, 189-217, 2009.
- [9] G. Ahmadi, *Self-similar solution of incompressible micropolar boundary layer flow over a semi-infinite plate*, Int. J. Engng. Sci, **14**, 639-646, 1976.
- [10] T. Hayat, M. Mustafa and S. Obaidat, *Soret and Dufour effects on the stagnation point flow of a micropolar fluid toward a stretching sheet*, Journal of Fluid Engineering, **133**, 1-9, 2011.
- [11] S. R. Mishra, S. Baag and D. K. Mohapatra, *Chemical reaction and Soret effects on hydro magnetic micropolar fluid along a stretching sheet*, Engineering Science and Technology, an International Journal, **19**, 1919-1928, 2016.
- [12] A. M. Rashad, S. Abbasbandy and A. J. Chamkha, *Mixed convection flow of micropolar fluid over a continuously moving vertical surface immersed in thermally and solutally stratified medium with chemical reaction*, Journal of Taiwan Institute of Chemical Engineers, **45**, 2163-2169, 2014.
- [13] A. A. A. Mahmoud, *Thermal radiation effects on MHD flow of a micropolar fluid over a stretching surface with variable thermal conductivity*, Physica A, **375**, 401-410, 2007.
- [14] Salawu, S. O. and Fatunmbi, E. O. *Dissipative Heat Transfer of Micropolar Hydromagnetic Variable Electric Conductivity Fluid Past Inclined Plate with Joule Heating and Non-Uniform Heat Generation*, Asian Journal of Physical and Chemical Sciences, **2**(1), 1-10, 2017.
- [15] Keimanesh, R. and Aghanajafi, *Effect of temperature-dependent viscosity and thermal conductivity on micropolar fluid over a stretching sheet*, Tehniki Vjesnik, **24**(2), 371-378. 2017.
- [16] E. O. Fatunmbi and A. Adeniyani, *MHD stagnation point-flow of micropolar fluid past a permeable stretching plate in porous media with thermal radiation, chemical reaction and viscous dissipation*, Journal of Advances in Mathematics and Comp Science, **26**(1), 1-19, 2018.
- [17] N. Casson, *Rheology of Disperse Systems in Flow Equation for Pigment Oil Suspensions of the Printing Ink Type*, *Rheology of disperse systems*, C. C. Mill, Ed., 84102, Pergamon Press, London, U. K. 1959.

- [18] K. Ahmad, Z. Hanouf and A. Ishak, *MHD Casson nanofluid flow past a wedge with Newtonian Heating*, Eur. Phys. J. Plus. **132**, 2017, <https://doi.org/10.1140/epjp/i2017-11356-5>
- [19] G. C. Shit and S. Mandal, *Entropy analysis on unsteady MHD flow of casson nanofluid over a stretching vertical plate with thermal radiation effect*, Int. J. Appl. Comput. Math, **6**(2), 1-22, 2020.
- [20] E. O. Fatunmbi and S. S. Okoya, *Quadratic Mixed Convection Stagnation-Point Flow in Hydromagnetic Casson Nanofluid over a Nonlinear Stretching Sheet with Variable Thermal Conductivity*, Defect and Diffusion, **409**, 95-109, 2021.
- [21] O. E. Omotola and E. O. Fatunmbi, *Magnetohydrodynamic radiative Casson fluid motion past a convectively heated and slippery non-linear permeable stretching plate*, Fepi-Jopas, **3**(1), 45-55, 2021.
- [22] W. Ibrahim, O. D. Makinde, *Magnetohydrodynamic Stagnation Point Flow and Heat transfer of Casson nanofluid past a stretching sheet with slip and convective boundary condition*, Journal of Aerospace Engineering, **30** 1-11. 2015.
- [23] T. Hayat, A. Shafiq, A. Alsaedi and S. Asghar, *Effect of inclined magnetic field in flow of third grade fluid with variable thermal conductivity*, AIP ADVANCES **5**, 087108, 2015.
- [24] Y. S. Daniel, Z. A. Aziz, Z. I., Ismail and F. Salah, *Entropy analysis in electrical magnetohydrodynamic (MHD) flow of nanofluid with effects of thermal radiation, viscous dissipation, and chemical reaction* Theoretical & Applied Mechanics Letters, **7**, 235242, 2017.
- [25] G. Aliy and N. Kishan *Effect of Electric Field on MHD Flow and Heat Transfer Characteristics of Williamson Nanofluid over a Heated Surface with Variable Thickness. OHAM Solution*, Journal of Advances in Mathematics and Computer Science, **30**, 1-23.2018.
- [26] A. Z. Rohni, S. Ahmad, A. I. Ismail and I. Pop, *Boundary layer flow and heat transfer over an exponentially shrinking vertical sheet with suction*, International Journal of Thermal Sciences, **64**, 264-272, 2013.
- [27] Z. Ullah, G. Zamana and A. Ishak, *Magnetohydrodynamic tangent hyperbolic fluid flow past a stretching sheet*, Chinese Journal of Physics, **66**, 258268, 2020.
- [28] Z. Mehmood, R. Mehmood and Z. Iqbal, *Numerical investigation of micropolar Casson fluid over a stretching sheet with internal heating*, Comm in Theoretical Phy,**67**(4), 443448, 2017.
- [29] Z. Iqbal, R. Mehmood, R. Azhara, and Z. Mehmood, *Impact of inclined magnetic field on micropolar Casson fluid using Keller box algorithm*. Eur. Phys. J. Plus, **132**, 1-13, 2017.
- [30] J. A. Gbadeyan, E. O. Titiloye and A. T. Adeosun, *Effect of variable thermal conductivity and viscosity on Casson nanofluid flow with convective heating and velocity slip*, Heliyon **6**, e03076, 2020.
- [31] I. L. Animasaun, E. Adebile and A. I. Fagbade, *Casson fluid flow with variable thermo-physical property along exponential stretching sheet with suction and exponentially decaying internal heat generation using homotopy analysis method*, Journal of the Nigerian Mathematical Society, **35** (1) 1-17, 2016.
- [32] M, Amjad, I. Zehra, S. Nadeem and N. Abba, *Thermal analysis of Casson micropolar nanofluid flow over a permeable curved stretching surface under the stagnation region*, Journal of Thermal Analysis and Calorimetry, 2020, <https://doi.org/10.1007/s10973-020-10127-w>
- [33] S. K. Jena and M. N. Mathur, *Similarity solutions for laminar free convection flow of a thermomicropolar fluid past a non-isothermal flat plate*, Int. J. Eng. Sci. **19** 1431-1439, 1981.
- [34] J. Peddieson, *An application of the micropolar model to the calculation of a turbulent shear flow*, Int. J. Eng. Sci., **10**, 23-32, 1972.

- [35] G. C. Layek, S. Mukhopadhyay and S. K. Samad, *Heat and mass transfer analysis for boundary layer stagnation point flow towards a heated porous stretching sheet with heat absorption/generation and suction/blowing*, Int Commun Heat Mass Transfer, **34**, 347-357, 2007.
- [36] T. E. Akinbobola and S. S. Okoya, *The flow of second grade fluid over a stretching sheet with variable thermal conductivity and viscosity in the presence of heat source/sink*, Journal of the Nigerian Mathematical Society **34**, 331342, 2015.
- [37] S. I. Opadiran and S. S. Okoya, *Importance of convective boundary layer flows with inhomogeneous material properties under linear and quadratic Boussinesq approximations around a horizontal cylinder*, Heliyon, **7**, e07074, 2021.
- [38] F. Mabood and K. Das, *Melting heat transfer on hydromagnetic flow of a nanofluid over a stretching sheet with radiation and second order slip*, Eur. Phys. J. Plus, **131**(3), 2016.
- [39] Mahanthesh, B., Gireesha, B. J., Gorla, R. S. R. and Makinde, O. D, *Magnetohydrodynamic three-dimensional flow of nanofluids with slip and thermal radiation over a nonlinear stretching sheet: a numerical study*, Neural Comput & Applic, **30**, 15571567, 2018.
- [40] B. S. Attili and M. L. Syam, *Efficient shooting method for solving two point boundary value problems*, Chaos, Solitons and Fractals, **35**(5), 895-903, 2008.
- [41] C. H. Chen, *Laminar mixed convection adjacent to vertical continuously stretching sheets*, Heat and Mass Transfer, **33**, 471-476, 1998.
- [42] M. Qasim, I. Khan, S and Shafie, *Heat transfer in a micropolar fluid over a stretching sheet with Newtonian heating*, Plos One, **8**(4), 1-6, 2013.
- [43] I. Kumar, *Finite element analysis of combined heat and mass transfer in hydromagnetic micropolar flow along a stretching sheet*, Computational Materials Science, **46**(4), 841-848, 2009.
- [44] Tripathy, R. S., Dash, G. C., Mishra, S. R. and Hoque, M. M. *Numerical analysis of hydromagnetic micropolar fluid along a stretching sheet embedded in porous medium with non-uniform heat source and chemical reaction*, Engineering Science and Technology, an International Journal, **19**, 15731581, 2016.

DEPARTMENT OF MATHEMATICS/STATISTICS, FEDERAL POLYTECHNIC, ILARO, NIGERIA

E-mail address: ephesus.fatunmbi@federalpolyilaro.edu.ng

DEPARTMENT OF MATHEMATICS, OBAFEMI AWOLOWO UNIVERSITY, ILE-IFE, NIGERIA

E-mail addresses: ssokoya@gmail.com and sokoya@oauife.edu.ng